

Noncollinear Maker's fringe measurements of second-order nonlinear optical layers

D. Faccio, V. Pruneri, and P. G. Kazansky

Optoelectronics Research Centre, Southampton University, Southampton, SO17 1BJ, UK

Received May 15, 2000

A novel technique for characterizing thin-film second-order nonlinearities with submicrometer resolution for the film's depth is proposed. This method is substantially a variation of the classic one-beam Maker's fringe technique and uses the second harmonic generated by two noncollinear fundamental beams. Compared with that for the one-beam case, this configuration reduces the coherence length of the process, thus increasing the resolution for the nonlinear depth measurements. The technique has been implemented on thermally poled silica samples, revealing the initial growth of the nonlinear region. © 2000 Optical Society of America

OCIS codes: 190.4400, 190.4160, 190.0190, 160.6030, 160.4330, 310.6870.

Since its first proposal,¹ the Maker's fringe technique (MFT) has been widely used to establish the effective second-order nonlinear coefficient (d_{eff}) and, when necessary, the thickness (L) of nonlinear materials, especially thin films. The technique is experimentally straightforward: A fundamental beam with frequency ω is focused onto the sample, and the second-harmonic (SH) power is recorded while the nonlinear thickness is varied, e.g., by rotation of the sample. From spacing and position of the SH peaks one can infer L , whereas d_{eff} can be estimated by comparison with a reference sample of known nonlinearity.² However, acceptable resolution for L is possible only when $L \geq l_c$, where l_c is the coherence length, i.e., the distance over which the SH field and the SH polarization wave (proportional to the square of the fundamental field) become π out of phase:

$$l_c = \frac{\pi}{|\Delta \mathbf{k}|} = \frac{\pi}{|\mathbf{k}_{2\omega} - \mathbf{k}_{\omega,1} - \mathbf{k}_{\omega,2}|}, \quad (1)$$

where $\mathbf{k}_{2\omega}$, $\mathbf{k}_{\omega,1}$, and $\mathbf{k}_{\omega,2}$ are the SH and the two fundamental wave vectors, respectively. Indeed, in the one-beam MFT the smallest measurable value for L is determined by the largest internal angle attainable in the sample, corresponding to total internal reflection for the SH at the back material-air interface. In silica glass, at 532-nm SH wavelength, this angle is 43.6° and indicates that a nonlinear region induced by thermal poling³ can be fully characterized only if $L > l_c \cos(43.6) \approx 18 \mu\text{m}$ ($l_c = 24 \mu\text{m}$), which often is not the case.⁴

A technique proposed by Pureur *et al.* overcomes this limitation by placing the sample between two glass prisms and thus eliminating the total internal reflection, making it possible to reach larger internal angles and correspondingly resolving smaller L .⁵ A further improved scheme, based on the same principle and using hemispherical lenses, has also been proposed.⁶ Here we propose a simple technique that can measure small nonlinear depths ($< 2 \mu\text{m}$) with high resolution ($< 0.5 \mu\text{m}$). Although our examples relate to silica, the contents of this Letter can be applied to any dispersive nonlinear thin film. Figure 1 is a schematic layout of the experimental geometry. Two identical fundamental beams, with field amplitudes $E_{\omega,1}$ and $E_{\omega,2}$ and with a relative external angle (Θ),

overlap in the sample, thus generating a polarization wave at 2ω , $P_{2\omega} \propto d_{\text{eff}}(E_{\omega,1}^2 + E_{\omega,2}^2 + 2E_{\omega,1}E_{\omega,2})$. The first two terms, with wave vectors $2\mathbf{k}_{\omega,1}$ and $2\mathbf{k}_{\omega,2}$ respectively, will generate so-called collinear SH fields, whereas the third term, with wave vector $\mathbf{k}_{\omega,1} + \mathbf{k}_{\omega,2}$, will generate a noncollinear SH field. It is worth observing that rigorously the SH fields (free waves) have slightly different propagation directions from those of the corresponding SH polarizations (bound waves).

As is true for the one-beam MFT, variation of the sample inclination angle (α) will change the nonlinear depth traversed by the incoming fundamental beams. The noncollinear SH power will oscillate periodically, reaching a maximum value at distances that are odd multiples of l_c . In the two-beam case, the projection of $\Delta \mathbf{k}$ along the SH field's internal propagation direction (z') is given by

$$\Delta k'(\Theta, \alpha) = \frac{4\pi}{\lambda} \left(n\left(\frac{\lambda}{2}\right) - \frac{n(\lambda)}{2} \{ \cos[\theta_1(\Theta, \alpha) - \gamma(\Theta, \alpha)] + \cos[\theta_2(\Theta, \alpha) - \gamma(\Theta, \alpha)] \} \right), \quad (2)$$

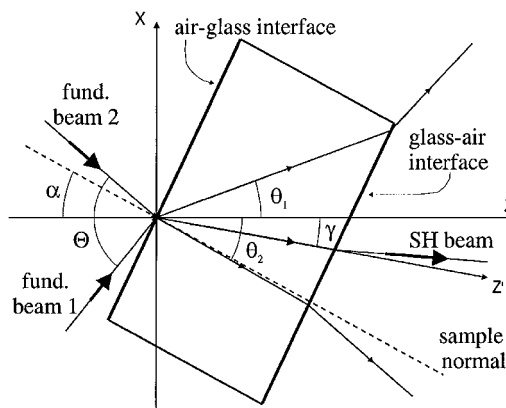


Fig. 1. Geometrical layout of the noncollinear Maker's fringe technique: The plane $x\hat{z}$ is defined as the lab reference system (taken so that \hat{z} is the symmetry axis of the two incident beams). θ_1 , θ_2 , and γ are the two fundamental (fund.) beam and SH internal propagation angles, respectively. α is the sample tilt angle, and Θ is the relative angle between the two input fundamental beams.

where λ is the fundamental wavelength and $\theta_1(\Theta, \alpha)$, $\theta_2(\Theta, \alpha)$, and $\gamma(\Theta, \alpha)$ are the two fundamental fields and the SH field's internal propagation angles, respectively (as shown in Fig. 1). They are defined in the laboratory reference system, taken such that \hat{z} is the symmetry axis of the two incident beams, by $\theta_1(\Theta, \alpha) = \sin^{-1}\{[\sin(\Theta/2 + \alpha)]/n_\omega\} - \alpha$, $\theta_2(\Theta, \alpha) = \sin^{-1}\{[\sin(\Theta/2 - \alpha)]/n_\omega\} + \alpha$, and $\gamma(\Theta, \alpha) = \sin^{-1}\{n_\omega/n_{2\omega} \sin[(\cos \theta_1 + \cos \theta_2)/2]\}$. The last expression is obtained from the boundary conditions for SH generation at the interface between a linear and a nonlinear medium, i.e., from the continuity of the magnetic and electric field tangential components.⁷

The overall normalized SH conversion efficiency ($\eta_{\text{SH}} = W_{2\omega}/W_\omega^2$), which is dependent on both α and Θ , is given by

$$\eta_{\text{SH}}(\Theta, \alpha) = \frac{2\omega^2}{\varepsilon_0 c_0^3 n_\omega^2 n_{2\omega}} \frac{u(\Theta, \alpha)}{\pi w_0^2} T_{2\omega} T_{\omega,1} T_{\omega,2} d_{\text{eff}}(\Theta, \alpha) \times \left| \int_{-\infty}^{\infty} \int_{-\infty}^{\infty} dx dy \left| \int_0^{\frac{L}{\cos \gamma(\Theta, \alpha)}} E_1 E_2 \exp[i\Delta k'(\Theta, \alpha)z'] dz' \right|^2 \right|, \quad (3)$$

where W_ω and $W_{2\omega}$ are the incident fundamental and output SH powers measured after the sample, $E_1 = E_{\omega,1}/\max(E_{\omega,1})$ and $E_2 = E_{\omega,2}/\max(E_{\omega,2})$ are the normalized fundamental fields, w_0 is their beam waist ($1/e^2$ intensity radius), n_ω is the material refractive index at ω and $n_{2\omega}$ at 2ω , ε_0 is the vacuum dielectric permittivity, and c_0 is the velocity of light in vacuum. The fundamental fields, E_1 and E_2 , are considered Gaussian—they depend on all three coordinates and on α through Snell's law—and plane waves (i.e., near-field approximation). $T_{\omega,1}$, $T_{\omega,2}$, and $T_{2\omega}$ depend on Θ and α and are the fundamental and the SH power Fresnel transmissivities, respectively. $u(\Theta, \alpha)$ is a projection factor for the beam area, which takes account of sample tilting. Finally, d_{eff} was taken with a square profile and $d_{\text{eff}}(\Theta, \alpha)$ is the projection of the excited tensor components along the direction normal to z' .

In the case of poled glass, the tensor will be that of a material with $C_{\infty v}$ symmetry, and we assume that the d_{eff} -tensor elements are related by $d_{33} = 3d_{31}$.⁸ For a fixed α , when the external angle Θ increases, both θ_1 and θ_2 increase and l_c decreases ($l_c = \pi/\Delta k'$). For $\Theta = 0^\circ$ ($\theta_1 = \theta_2$) we have the one-beam case, but, for example, for $\Theta = 90^\circ$, l_c has an average value (over the possible α) that is smaller than $2 \mu\text{m}$ in silica glass, in contrast to the $24\text{-}\mu\text{m}$ value for collinear, i.e., one-beam, interaction. This means that nonlinear region depths as small as $l_c \cos(43.6) \approx 1.5 \mu\text{m}$ can be measured. A comparison of one-beam and noncollinear MFT (with $\Theta = 90^\circ$) is shown in Fig. 2 for three values of L (5, 9, and $14 \mu\text{m}$). One-beam MFT produces nearly identical curves [Fig. 2(a)], which, instead, become easily distinguishable in the noncollinear case [Fig. 2(b)].

The experiments were carried out with a Q -switched and mode-locked Nd:YAG laser as the fundamental source. The polarization is controlled with a Glan-Thompson polarizer followed by a half-wave

plate. The pulses are then split by a 50% beam splitter before being focused onto the sample. The SH signal is measured with a photomultiplier tube after the fundamental wavelength is reflected by an interferometric filter. The samples used were $25 \text{ mm} \times 25 \text{ mm} \times 0.1 \text{ mm}$ HeraSil 1 slides (from Heraeus). Five slides (A, B, C, D, and E) were thermally poled in air at 4 kV and 280°C for 5, 10, 20, 30, and 45 min, respectively (see Table 1). The Maker's fringes from all samples were initially measured with the one-beam configuration, but they all yielded indistinguishable curves with a maximum at the same angle ($\approx 60^\circ\text{--}62^\circ$). As we have already said [see Fig. 2(a)], this result indicates that all the poled samples have $L < 18 \mu\text{m}$. Measuring the Maker fringe modulation of the noncollinear SH enables us to improve the resolution, which shows that thickness L is less than $18 \mu\text{m}$ for all samples and its dependence on poling time. Figure 3 shows, as examples, the curves obtained for samples B (10-min poling) and D (30-min poling) along with the best fit given by our

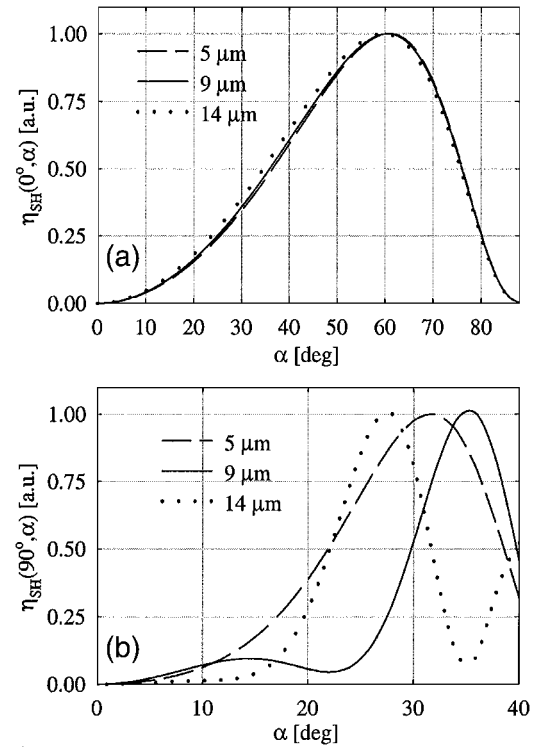


Fig. 2. Comparison of (a) a one-beam or collinear MFT ($\Theta = 0^\circ$) and (b) a two-noncollinear-beam MFT ($\Theta = 90^\circ$). Solid curve and dotted curves, values of L . Note the different scale for the angle axis.

Table 1. Summary of Measured Values^a

| Sample | Poling Time (min) | L (μm) | d_{33} (pm/V) |
|--------|-------------------|-----------------------|-----------------|
| A | 5 | 4 | 0.54 |
| B | 10 | 4 | 0.55 |
| C | 20 | 6.8 | 0.35 |
| D | 30 | 8 | 0.26 |
| E | 45 | 10.8 | 0.23 |

^a L is the nonlinear thickness and d_{33} is the second-order nonlinear optical coefficient.

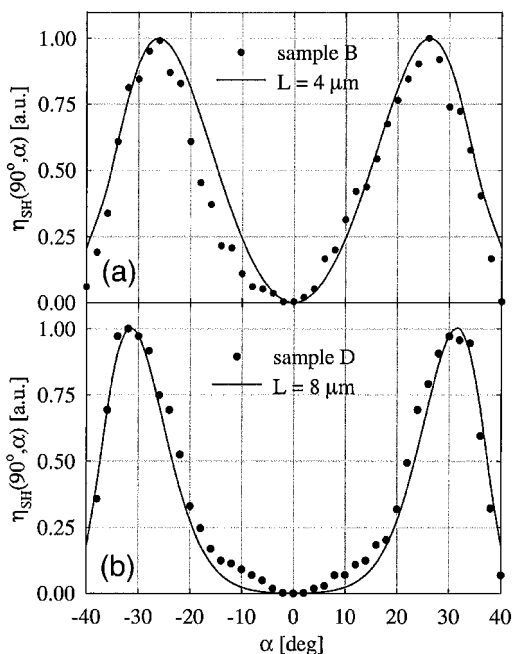


Fig. 3. Experimental results: normalized SH conversion efficiency (η_{SH}) as a function of the external tilt angle (α) for noncollinear fundamental beams with $\Theta = 90^\circ$. Filled circles, experimental values obtained for two samples from Table 1. Solid curves, best calculated fits.

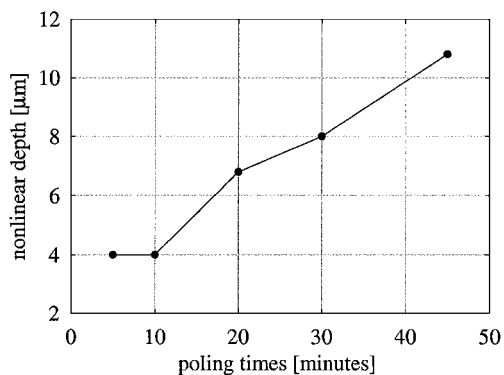


Fig. 4. Experimental results: measured nonlinear depth as a function of poling time for the five measured samples of Table 1.

calculations. Repeated measurements of the samples have always produced similar results, within $0.2 \mu\text{m}$, for L .

Our values of nonlinear thickness agree well with those obtained with other methods, such as chemical etching.^{4,9,10} The observed nonlinear growth of depth with poling time (Fig. 4) also agrees with that reported previously.^{4,9} Once L has been evaluated by the noncollinear MFT, one can perform a collinear SH experiment to measure the nonlinear optical coefficient by using a reference sample (e.g., quartz). Table 1 shows the values for L and d_{33} , assuming that $d_{33} = 3d_{31}$. Poling times longer than those in Table 1 produce larger nonlinear depths and therefore more pro-

nounced modulations of the SH signal. However, we noted that in this case the noncollinear Maker fringes become rather noisy, especially at large tilt angles. This is probably due to the fact that local nonuniform nonlinear regions (within the poled layer) with dimensions of the order of the coherence length ($\approx 2 \mu\text{m}$ for $\Theta = 90^\circ$) may interferometrically contribute to the SH signal. One can reduce this noise by decreasing Θ , thus increasing l_c , so the effects that are due to possible nonuniform nonlinear distributions are averaged. In fact, for increasing L , Θ can be reduced, and when $L \geq l_c$ it is convenient to use the one-beam MFT (i.e., $\Theta = 0^\circ$). One can also address uncertainty in the value of L by carrying out cross measurements at different values of Θ .

In conclusion, we have used noncollinear SH generation to increase MFT resolution and to characterize thin (less than $18\text{-}\mu\text{m}$) second-order nonlinear layers. The technique has been demonstrated on a series of thermally poled silica glass slides. A complete expression has been derived for the noncollinear SH conversion efficiency and then used to fit the experimental data. The results agree with those obtained with other methods. The main advantages of the new technique are that it is nondestructive, an easy-to-implement modification of the classic one-beam MFT, and extremely precise and can be tailored, by a change of Θ , to characterize second-order nonlinear films of any kind.

This research was supported by Pirelli Optical Components. D. Faccio's e-mail address is dfaf@orc.soton.ac.uk.

References

1. P. D. Maker, R. W. Terhune, M. Nisenhoff, and C. M. Savage, *Phys. Rev. Lett.* **8**, 21 (1962).
2. J. Jerphagnon and K. Kurtz, *J. Appl. Phys.* **41**, 1667 (1970).
3. R. A. Myers, N. Mukherjee, and S. R. J. Brueck, *Opt. Lett.* **16**, 1732 (1991).
4. V. Pruneri, F. Somoggia, G. Bonfrate, P. G. Kazansky, and G. M. Yang, *Appl. Phys. Lett.* **74**, 2423 (1993).
5. D. Pureur, A. C. Liu, M. J. F. Digonnet, and G. S. Kino, *Opt. Lett.* **23**, 588 (1998).
6. Y. Quiquempois, G. Martinelli, F. Valentin, P. Bernage, P. Niay, and M. Douay, in *Bragg Gratings, Photosensitivity, and Poling in Glass Waveguides*, E. J. Friebele, R. Kashyap, and T. Erdogan, eds., Vol. 33 of OSA Trends in Optics and Photonics Series (Optical Society of America, Washington, D.C., 2000), paper ThE21, pp. 106–108.
7. N. Bloembergen and P. S. Pershan, *Phys. Rev.* **128**, 606 (1962).
8. P. G. Kazansky and P. St. J. Russell, *Opt. Commun.* **110**, 611 (1994).
9. T. G. Alley and S. R. J. Brueck, *Opt. Lett.* **23**, 1170 (1998).
10. A. Triques, C. Cordiero, V. Balestrieri, B. Lesche, W. Margulis, and I. Carvalho, *Appl. Phys. Lett.* **76**, 2496 (2000).